

UDC 539.1.09

## LUMINESCENT SILICA NANOPARTICLES: MORPHOLOGY AND SYNTHESIS METHODS

A. Zhanbotin

L.N. Gumilev Eurasian National University, 5 Munaitpasov Str. Astana 010008, Kazakhstan, g.armani@mail.ru

*Luminescent, photostable, and easily functionalized silica nanoparticles (NPs) have been widely used for biochemical sensing, time-resolved fluoroimmunoassay, imaging of blood vessels, and bioanalytical assays. These NPs are typically generated by incorporating different emission centers, such as organic/inorganic fluorophores, quantum dots, or lanthanides, into the silica matrix. The current article reviews different researches of Luminescent colloidal silica nanoparticles for period of last couple years and shows how their properties can be used in different applications. Main works based on using tetraethylorthosilicate (TEOS) to grow nanoparticles of mesoporous silica. The main method to prepare them was Stober basic route.*

**Keywords:** luminescent, silica nanoparticles, emission centers, fluorophores, Stober basic route.

### Introduction

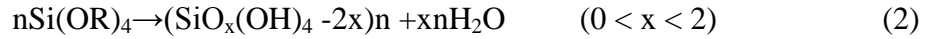
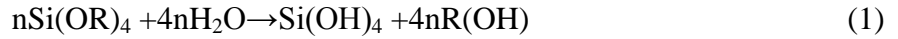
Luminescent nanoparticles are becoming more and more important in the field of biosensors and bioimaging [1,2], leading to improvements in sensitivity, selectivity, and multiplexing capacity [3] over conventional fluorophores. Key features for their actual use for in vitro and in vivo applications are the intensity of their optical emission, the efficiency of their surface fictionalization for molecular recognition, and their low toxicity. For all these reasons, silica nanoparticles seem to be an interesting choice [4] because of easy control of their surface ligands and biocompatibility [5]. Moreover, the possibility of having a cheap, fast, and reliable production process would also be desirable. Silica spheres can be obtained by condensation of TEOS by a Stober basic route [6] or by an acidic route [7,8]. Several strategies have been recently developed to make such spheres luminescent by the incorporation of organic or inorganic emission centers, such as common dyes [9], rare-earth elements [9,10], or quantum dots [11,12]. Most of these procedures allow reaching a strong photoluminescence (PL) emission but unfortunately require multiple processing steps and the use of expensive or toxic fluorophores.

The sol-gel polymerization of silicon alkoxides has been widely used for the preparation of a variety of silica-based materials, including monoliths, thin films, small particles, and porous materials. Thus, the mechanism of the sol-gel process has been extensively studied and investigated during the past decades [13,14].

Uchino, T., Kurumoto, N., Sagawa N. have studied [15] the PL characteristics of silica gels with different microscopic morphology, which are prepared by acid- and base-catalyzed hydrolysis of tetraethylorthosilicate in ethanol solution. All the gels show visible PL emission peaking at ~420nm after annealing the sample at ~200°C in air; however, the PL intensity and decay kinetics are strongly dependent on the microstructure and porosity of the initial gels. The annealing-induced PL intensity increases with decreasing porosity of the initial gels, whereas the PL decay dynamics tends to deviate from a pure exponential trend as the porosity of the initial gels becomes higher. These results indicate that the formation, stabilization, and radiative recombination process of the emission centers that are created during annealing are influenced by the microscopic morphology of the gels. These experimental results are interpreted in terms of the formation mechanism of the visible emission center in silica-based nanostructure materials proposed recently.

Although all the as-prepared gels were hardly luminescent, substantial PL signals were

Observed in blue spectral region after annealing the gels at  $\sim 200^{\circ}\text{C}$ . A simplified description of the hydrolysis-polycondensation of silicon alkoxides is as follows:



where:  $(\text{SiO}_x(\text{OH})_{4-2x})_n + xn\text{H}_2\text{O}$  is a silica gel of as yet unspecified structure. The as-prepared gel compound contains a number of surface OH groups and pore liquid and is hence often referred to as aquagel or hydrogel. Many factors, such as the water/alkoxide molar ratio, pH, and the steric volume of organic chains, can influence the surface and pore structures of aquagels, allowing them to obtain various polymeric gel structures, e.g., linear, entangled chains, clusters, and colloidal particles, after removal of the pore liquid [16]. There are several ways to remove the pore liquid from aquagels. Conventional drying of an aquagel in a drying oven or furnace results in a xerogel, often accompanied by further polycondensation and large shrinkage (and mostly destruction) of the initially uniform gel body. When the pore liquid is removed by supercritical drying (or by freeze-drying), an aerogel (or a cryogel) is obtained [17].

It has been found, that the drying process not only dries wet gels but also can lead to the creation of PL centers [18]. Visible PL under ultraviolet (UV) excitation has been reported recently from various types of sol-gel derived dry silica gels, including xerogels [18-20], aerogels [21], mesoporous silicas [22], and hybrid organic/inorganic gels [23-27].

Similar visible PL emission has been observed in other silica-based nanostructured materials, such as silica nanoparticles [28] and nanowires [29,30] both of which are not prepared by a sol-gel route but by gas-phase reactions. It is interesting to note that the PL emission from these silica based materials has several common features irrespective of the starting materials, preparation processes, and drying procedures. First, the PL peak wavelength is generally located

In the blue wavelength region at  $\sim 420\text{nm}$  [18] and the corresponding PL excitation (PLE) peak wavelength are observed at  $\sim 350\text{nm}$  [17,20,24,28,30]. Second, the PL decay is characterized by a highly nonexponential function with a time scale of several tens of nanoseconds at room temperature [12,27,28]. Third, the PL emission is generally increased when the materials are annealed at  $\sim 200\text{-}400^{\circ}\text{C}$ , where higher temperature annealing at  $T > \sim 600^{\circ}\text{C}$  almost completely quenches the PL emission [18-20,26,28]. These results strongly suggest that common emission centers are responsible for the blue PL from these silica-based materials. However, the identification of the emitting centers pertaining to the blue PL emission remains an open question. Several possible mechanisms, including carbon impurity mechanism [23] and defect-related mechanisms [24,28] have been proposed to explain the PL phenomena.

It was investigated [28] effect of microstructure and porosity of silica gel monoliths on the resulting PL properties. The highest PL intensity was obtained when the silica gel with less porosity was annealed. From the experimental results, it was proposed that the development of PL is related to the condensation reaction of interacting or internal silanol groups, leading to the formation of possible emission centers. It has also found that the decay process of the annealed gels is described by a double-exponential function and that the slow-decay component is especially influenced by the microscopic structures of the initial gels. The gel with larger pores unambiguously has a slow-decay component, whereas the gel with less porosity tends to show a pure exponential-like decay profile. Thus, it was concluded that the slow-decay component results from surface-related trapping and detrapping processes and that the fast-decay component represents the effective radiative lifetime of the electron-hole recombination process of the emission centers.

The synthesis and characterization of colloidal mesoporous silica (CMS) functionalized with vinyl-,benzyl-,phenyl-,cyano-,mercapto-,aminopropyl-or dihydroimidazol emoieties is reported by Johannes Kobler, Karin Möller, and Thomas Bein [31]. Uniform mesoporous particle sranging size

from 40 to 150nm are generated in a co-condensation process of TEOS and organotriethoxysilanes (RTES) in alkaline aqueous media containing triethanolamine (TEA) in combination with cetyltrimethylammoniumchloride (CTACl) serving as a structure-directing agent. The materials are obtained as colloidal suspensions featuring long-term stability after template removal by ion exchange with an ethanolic solution of ammonium nitrate or HCl. The spherical particles exhibit a wormlike pore system with defined pore sizes and high surface areas. Samples are analyzed by a number of techniques including TEM, SEM, DLS, TGA, Raman, and cross-polarized  $^{29}\text{Si}$ -MAS NMR spectroscopy, as well as nitrogen sorption measurements. It was demonstrated that co-condensation and grafting methods result in similar changes in the nitrogen adsorption behavior, indicating a successful internal lining of the pores with functional groups through both procedures.

Colloidal mesoporous silica (CMS) was prepared in the form of nonfunctionalized pure-silica MCM-like material and as functionalized mesoporous materials carrying seven different organic groups (R) in the pore walls. The materials were obtained as colloidal suspensions with relatively uniform particle sizes between 40 and 150 nm. TEOS and RTES form the MCM-like material in combination with CTMA as structure directing agent in a co-condensation process. This  $S^{+}$  assembly takes place in an alkaline aqueous medium, with TEA as basic reactant. TEA can also act as a complexing agent that retards the hydrolysis of the alkoxides. It was assumed that in these reactions the uncomplexed TEOS is hydrolyzed upon contact with water, followed by forming the seeds of the mesostructure. The large excess of TEA probably keeps the seeds separated from each other during the condensation process giving rise finally to a large number of particles with relatively small diameters.

The synthetic approach presented here can serve as a general method for the preparation of both colloidal mesoporous silica spheres CMS and functionalized colloidal suspensions of nanoscale mesoporous materials with high yields from concentrated solutions. Narrow particle size distributions in the range of about 40 to 150nm were established with dynamic light scattering (DLS) measurements and electron microscopy before and after template extraction. Discrete nanoscale mesoporous particles with functionalized pore surfaces result when adding functional organoalkoxysilanes directly to the initial silica precursor solutions, or alternatively, when organoalkoxysilanes are grafted to the pore surfaces in a second step. The comparison of both methods with nitrogen sorption analysis and spectroscopic data demonstrates that the functional groups are located at the inner surfaces of the mesoporous channel systems, while the latter retain large surface areas and significant pore volumes.

Triple-dye-doped fluorescence resonance energy transfer (FRET) silica NPs were prepared [32] via a modified Stober synthesis method. The three tandem dyes were chosen carefully to allow for efficient FRET, fluorescein isothiocyanate (FITC), rhodamine 6G (R6G), and reliable oxygen (ROX) were employed in their model construction because of their effective spectral overlapping. In the triple-dye-doped NPs, FITC was used as a common donor for R6G and ROX, while R6G acted as both an acceptor for FITC and a donor for ROX. To prepare the NPs, the three types of amine reactive dye molecules were first covalently linked to the silane coupling agent APTS [(3-aminopropyl)-triethoxysilane]: FITC-SE [5-(and-6)-carboxyfluorescein, succinimidylester], R6G-SE [5-carboxyrhodamine 6G, succinimidylester], and ROX-SE [6-carboxy-X-rhodamine, succinimidylester] were individually dissolved in 1.5mL of anhydrous DMF, combined with an excess of APTS at a molar ratio of dye to APTS of 1:2, and stirred under a dry nitrogen atmosphere for 24 h in the dark. Second, the three APTS-dye conjugates were mixed at desired ratios and added to a clean glass reaction vessel containing 16.75mL of pure ethanol and 1.28mL of ammonium hydroxide (28.8%). The mixture was stirred for 24 h. TEOS (0.71mL) was added afterward and stirred for another 24 h. After the reaction, the samples were centrifuged at 14 000rpm for 30 min to collect the silica NPs. The NPs were further washed with ethanol and deionized water by centrifugation and decantation several times to remove the unreacted chemicals. During their initial preparation process, TEOS was introduced immediately after APTS-dye conjugates were added to

the basic ethanol solution. However, it was found that there was rather low FRET efficiency between the dyes. The peak intensity ratios (measured at 520, 550, and 605nm, respectively) of the triple-dye-doped NPs (dye doping ratio ) 1:1:1) are 1:0.8:0.4. ROX dye exhibits a weak fluorescence signal because of the low FRET efficiency. It is known that FRET is mediated by a dipole-dipole coupling between chromophores and the FRET efficiency is proportional to the inverse sixth power of the distance between the chromophores.

The FRET efficiency between an R-naphthyl energy donor group and a dansyl energy acceptor group has been found to be 100% at a distance of 1.2 nm and 16% at 4.6 nm. The low FRET efficiency implies a large separation distance between the dyes encapsulated inside the NPs. Their reasoning is based on the following: 1) the APTS-dye conjugates must be hydrolyzed to be incorporated into the silica matrix, it is likely that the hydrolysis reaction rates of each APTS-dye conjugates are different, so the three dyes are encapsulated into different silica layers, and the spacer shells in between reduce the FRET efficiency; 2) the hydrolysis rate of APTS is five times slower than that of TEOS because of the electron-donating capacity of the alkyl group, and siloxane bond formation is much faster than the hydrolysis step; therefore, TEOS could be converted entirely to silica NPs before a large number of dyes are housed inside. The FRET efficiency is low because of a large portion of the dyes not being incorporated into the particles during synthesis or because of physical separation of the FRET pairs. To address these challenges, the three APTS- dye conjugates were mixed and prehydrolyzed for 24h before beginning the colloid formation by the addition of TEOS. This strategy not only ensures a greater amount and equal opportunity of the dyes incorporated during NP synthesis but also allows the formation of small dimers or oligomers between the APTS-dye conjugates. The possible formation of such dye clusters made fluorophores covalently attached to one another and shortened the distance between them to the benefit of the FRET efficiency. However, it should be mentioned that the close proximity of the fluorophores might also lead to self-quenching between identical species, so the dye-loading amount was experimentally optimized to find a compromise between minimal self-quenching and maximal FRET efficiency.

## Conclusions

In summary, FRET has been reported as a tool to construct barcoding silica NPs for multiplexed signaling. By varying the ratio of the three tandem dyes co encapsulated into the silica NPs, the NPs exhibit multicolor under one single wavelength excitation. The NPs can be made with different sizes via easy control of synthetic parameters. They are uniform, exhibit high fluorescence intensity and excellent photostability, and can be labeled easily with biomolecules such as proteins and nucleic acids. One other potential advantage of FRET NPs is that by optimizing the amount of dye molecules in a NP, the emission spectrum can be tuned so that only the longest-wavelength dye will exhibit significant fluorescence at a short-wavelength excitation. This feature will overcome the challenge of the small Stokes shift of many organic dyes, enabling the NPs to be detected in samples with significant Rayleigh/Raman scattering or with endogenous fluorescent compounds. It is also noteworthy that the covalent trichromophoric labeling approach can be further extended to more than three chromophores; the FRET NP strategy can be applied to any energy transfer dye series.

The significance of this study lies in that it provides highly fluorescent and photostable barcoding NPs that permit simultaneous and sensitive detection of multiple targets as well as opens up a new perspective in the design of multifunctional structures based on silica NPs, which have seen a variety of interesting applications in the past few years.

## References:

1. Tansil N. C., and Gao Z., *Nanotoday* (2006). 1, p.28.
2. Seydack M., *Biosens. Bioelectron.* (2005). 20, p.2454.

3. Wang L., O'donoghue M.B., and Tan W., (2006). *Nanomedicine* 1, p.413.
4. Tan W., Wang K., He X., et al. *Med.Res.Rev.* (2004). 24, p.621.
5. Jin Y., Kannan S., Wu M., and Zhao J. X., *Chem. Res.* (2007). *Toxicol.* 20, p.1126.
6. Stober W., Fink A., and Bohn E., *J. Colloid Interface* (1968). *Sci.* 26, p.62.
7. Karmakar B., De G., and Ganguli D., *J. Mater. Chem.* (2000). 10, p.2289.
8. Karmakar B., De G., and Ganguli, D., *J. Non-Crystalline Solids* (2000). 272, p.119.
9. Sokolov I., Kievsky Y.Y., J. M., *Small* (2007). 3, p.419.
10. De Dood M.J., Berkhout A.B., Van Kats C.M., et al. *Chem. Mater.* (2002). 14, p.2849.
11. Moran C.E., Hale G. D., and Halas N.J., *Langmuir* (2001). 17, p.8376.
12. Chan Y., Zimmer, J.P., Stroh M., et al. *Adv. Mater* (2004). 16, p.2092.
13. Hench L.L., West J.K., *Chem. ReV.* (1990), 90, p.33.
14. Brinker C.J., Scherer G.W., *Sol-Gel Science, Processing*; Academic Press: San Diego, CA, (1990).
15. Uchino T., Kurumoto N., Sagawa N., *Phys. ReV. B* (2006) 73, p.233.
16. Schaefer D.W., *Science* (1989). 243, p.1023.
17. Pierre A.C., Pajonk G.M., *Chem. ReV.* (2002). 102, p.4243.
18. Yoldas B.E., *J. Non-Cryst. Solids* (1992). 147&148, p.614.
19. Garcia J., Mondragon M.A., Tellez C., Campero A., Castano V.M., *Mater. Chem. Phys.* (1995). 41, p.15.
20. Lin J., Baerner K., *Mater. Lett.* (2000). 46, p.86.
21. Ayers M.R., Hunt A.J., *J. Non-Cryst. Solids* (1997). 217, p.229.
22. Liu Y.L., Lee W.Z., Shen J.L., Lee Y.C., Chang P.W., Cheng C.F., *Appl. Phys. Lett.* (2004) 85, p.6350.
23. Green W.H., Le K.P., Grey J., Au T.T., Sailor M., *J. Science* (1997) 276, p.1826.
24. Carlos L.D., de Zea Bermudez V., SaFerreira R.A., Marques L., Assuncao M., *Chem. Mater.* (1999) 11, p.581.
25. Brankova T., Bekiari V., Lianos P., *Chem. Mater.* (2003) 15, p.1855.
26. Han Y., Lin J., Zhang H., *Mater. Lett.* (2002) 54, p.389.
27. Stathatos E., Lianos P., Orel B., Surca Vuk A., Jese R., *Langmuir* (2003) 19, p.7587.
28. Nakazaki et al. *J. Phys. Chem. C*, (2008). **V. 112**, No. 29.
29. Yu D.P., Hang Q.L., Zhang H.Z., Bai Z.G., Wang J.J., Zou Y.H., Qian W., Xiong G.C., Feng S.Q., *Appl. Phys. Lett.* (1998) 73, p.3076.
30. Chen Z., Wang Y.X., He H.P., Zou Y.M., Wang J.W., Li Y., *Solid State Commun.* (2005). 135, p.247.
31. Kobler J., Möller K., and Bein T., *American Chemical Society*, (2008). **V. 2**, no. 4, p.791
32. Lin Wang and Weihong Tan. *Nano Lett.* (2006). **V. 6**, No. 1